

Electrochemical Deposition–Stripping Analysis of Molecules and Proteins by Online Electrochemical Flow Cell/Mass Spectrometry

Vitaly Gutkin, Jenny Gun, and Ovidia Lev*

Laboratory of Environmental Chemistry, The Chemistry Institute, The Hebrew University of Jerusalem, Jerusalem, 91904, Israel

A methodology for online preconcentration of analytes and their subsequent electrochemically induced delivery to an online electrospray mass spectrometer is introduced. The approach is based on electrodeposition of an active metallic layer, silver deposit in this particular case, subsequent specific accumulation of the target analyte by electrochemical or chemical means onto the active layer, and finally oxidative electrostripping of the conductive layer along with the supported analyte to an online mass spectrometer. We demonstrate the new concept by selective electrochemical deposition of homocysteine and other organothiols directly on the working electrode of a miniature flow cell. The same approach was extended to the conjugation of the target analyte (avidin as a test case) to a thiolated ligand (biotin in this case) that was electrodeposited on the silver coated surface. Electrostripping of the silver dissolves the target species and allows their delivery to an online ESI-MS. Furthermore, the dissolved silver ions promote ionization, and its characteristic isotopic pattern assists in the identification of the target analyte.

Solid sample enrichment techniques are now increasingly used in combination with mass spectrometry. Their use is no longer restricted to increasing method sensitivity by accumulation of the target analytes prior to introduction to the mass spectrometer (MS). Many other applications of solid adsorption and extraction are aimed at overcoming the inherent limitations of coupling chromatography and matrix assisted laser desorption/ionization (MALDI) or electrospray mass spectrometry. Solid phase extraction is now increasingly used for rough fractionation (i.e., obtaining crude separation) or matrix cleanup and particularly to get rid of surfactants or excess electrolyte (i.e., reduce ionic strength). Solid phase enrichment is also frequently used to change the solvent to a MS compatible solvent. Better specificity, and at times even speciation, can be achieved by selective uptake of the target species or by adsorption followed by (more efficient and selective) target molecule tagging. In some cases, adsorption on an addressable (chip) array of different specific ligating agents can be used instead of chromatographic separation for screening or fast multicomponent analysis. Recent reviews, which naturally em-

phasize surface enhanced laser desorption/ionization-time-of-flight mass spectrometry, SELDI-TOF, have been published recently.^{1–4} The transformation of this successful technology to electrospray interfaced mass spectrometers is more challenging because it requires a method to address individual spots on the surface. Electrochemistry may provide such spatial resolution and a generic method for electrochemically induced delivery of analytes to an ESI-MS is presented here, though it has still to be generalized to a microarray format.

Electrochemical preconcentration techniques are compatible with contemporary trends in sample introduction to mass spectrometers involving increased instrumental automation, miniaturization, and use of microfluidics. Combined electrochemical flow cell and mass spectrometry (EC/MS) techniques were recently reviewed.^{5–8} EC/MS techniques and particularly those involving electrospray mass spectrometry (EC/ESI-MS) are used for identification of electrochemical transformations of analytes (for recent articles see, for example refs 9–29) and tagging or oxidation of chemical analytes to enhance ESI-MS sensitivity.^{30,31} Less was done in the area of peptide and protein research, but notably EC/ESI-MS was used to study electrochemical transformations³² and cleavage^{33,34} and for tagging^{35–40} of peptides and proteins prior to ESI-MS analysis. An interesting recent electrochemical tagging, which is somewhat relevant to our approach, includes the anodization of sacrificial copper anodes to generate copper ions that complex (8-hydroxyquinoline or bathocuproine) copper chelating agents⁴¹ or peptides.⁴²

- (1) Merchant, M.; Weinberger, S. R. *Electrophoresis* **2000**, *21*, 1164–1177.
- (2) Baggerly, K. A.; Morris, J. S.; Coombes, K. R. *Bioinformatics* **2004**, *20*, 777–785.
- (3) Schaub, S.; Wilkins, J.; Weiler, T.; Sangster, K.; Rush, D.; Nickerson, P. *Kidney Int.* **2004**, *65*, 323–332.
- (4) Wulfkühle, J. D.; McLean, K. C.; Paweletz, C. P.; Sgroi, D. C.; Trock, B. J.; Steeg, P. S.; Petricoin, E. F. *Proteomics* **2001**, *1*, 1205–1215.
- (5) Zhou, F. M. *Trends Anal. Chem.* **2005**, *24*, 218–227.
- (6) Permentier, H. P.; Bruins, A. P.; Bischoff, R. *Mini-Rev. Med. Chem.* **2008**, *8*, 46–56.
- (7) Diehl, G.; Karst, U. *Anal. Bioanal. Chem.* **2002**, *373*, 390–398.
- (8) Karst, U. *Angew. Chem.* **2004**, *43*, 2437–2478.
- (9) Lohmann, W.; Dotzer, R.; Gutter, G.; Van Leeuwen, S. M.; Karst, U. *J. Am. Soc. Mass Spectrom.* **2009**, *20*, 138–145.
- (10) Mautjana, N. A.; Estes, J.; Eyler, J. R.; Bräijter-Toth, A. *Electroanalysis* **2008**, *20*, 2501–2508.
- (11) Mautjana, N. A.; Estes, J.; Eyler, J. R.; Bräijter-Toth, A. *Electroanalysis* **2008**, *20*, 1959–1967.
- (12) Lohmann, W.; Karst, U. *Anal. Bioanal. Chem.* **2008**, *391*, 79–96.
- (13) Nozaki, K.; Kitagawa, H.; Kimura, S.; Kagayama, A.; Arakawa, R. *J. Mass Spectrom.* **2006**, *41*, 606–612.

* To whom correspondence should be addressed. E-mail: ovidia@vms.huji.ac.il.

Anodic (and less often cathodic) stripping analysis of metal cations as well as other analytes is amply exploited in modern analytical electrochemistry,⁴³ and this approach was adopted for EC/MS techniques. Indeed, coupled electrochemical flow cell with online ICPMS (ICP is an acronym for inductively coupled plasma) has already reached maturity, largely due to the efforts of the groups of Caruso,^{44–47} van Berkel,^{48–50} and Zhou.^{4,51–54}

Nyholm and co-workers have recently shown that the methods are not confined to metal cations, and that EC preconcentration on an electrochemically deposited anion exchange polypyrrole film can be used for EC/ICPMS analysis of bromide in aqueous systems.⁵⁵ Furthermore, EC/MS is not confined to ICPMS analysis. Nyholm and co-workers⁵⁵ demonstrated that the method can be used for preconcentration of ferricyanide on polypyrrole and its subsequent desorption to an online ESI-MS, though again, this process targets inorganic ions.

The only article that we have found that deals with electrochemically modulated preconcentration of organic analytes is van Berkel's article on the determination of the breast cancer drug tamoxifen.⁵⁶ Negative electrode bias resulted in accumulation of the positively charged compound (a tertiary amine) on the glassy carbon electrode, and positive bias released the analyte to a stream flowing to an online mass spectrometer. The method however is not compound-selective, and all hydrophobic and charged analytes would accumulate on the electrode, which is an asset in some cases but may constitute a drawback when better selectivity is desirable.

Here we introduce a proof of principle of a generic EC enrichment approach prior to ESI-MS analysis. The principle of the proposed method is based on the deposition of a silver layer on an electrode, subsequent attachment of an analyte to the deposit either directly or through a thiol tethered chelating agent, and finally, after an additional preconcentration step of the target analyte, the silver ions, the chelating agent, and the analyte are all desorbed to the mass spectrometer. The preconcentration can be tuned to be more or less selective depending on the choice of the chelating ligand.

EXPERIMENTAL SECTION

Electrospray Ionization Mass Spectrometry (ESI-MS).

Mass spectrometry was conducted by a Finnigan (San Jose, CA) LCQ Classic ion trap mass spectrometer equipped with an electrospray ionization interface. The ESI was operated in the positive ion mode. Sheath gas flow rate was set to 70 (arbitrary units), the spray voltage, capillary source temperature, and capillary voltage were optimized for each application. For the organothiol, the preconcentration/stripping tests spray voltage was 3.0 kV, capillary source temperature was 130 °C, and capillary voltage was 30 V. The mass range was 50–500 *m/z*. For the avidin determination tests, the spray voltage was 4.5 kV, capillary temperature was set to 180 °C, and capillary voltage was 60 V. The mass range was 500–4000 *m/z*. The analyzer was operated at a background pressure of 2×10^{-5} Torr. Helium was introduced to improve the ion trapping efficiency. The spectral

(14) Liljegren, G.; Dahlin, A.; Zettersten, C.; Bergquist, J.; Nyholm, L. *Lab Chip* **2005**, *5*, 1008–1016.
 (15) Van Leeuwen, S. M.; Blankert, B.; Kauffmann, J. M.; Karst, U. *Anal. Bioanal. Chem.* **2005**, *382*, 742–750.
 (16) Kertesz, V.; Van Berkel, G. J. *J. Solid State Electrochem.* **2005**, *9*, 390–397.
 (17) Van Berkel, G. J.; Kertesz, V.; Ford, M. J. *J. Am. Soc. Mass Spectrom.* **2004**, *15*, 1755–1766.
 (18) Arakawa, R.; Yamaguchi, M.; Hotta, H.; Osakai, T.; Kimoto, T. *J. Am. Soc. Mass Spectrom.* **2004**, *15*, 1228–1236.
 (19) Yamaguchi, M.; Mizooka, Y.; Osakai, T.; Kimoto, T.; Arakawa, R. *Bunseki Kagaku* **2004**, *53*, 547–553.
 (20) Modestov, A. D.; Gun, J.; Savotina, I.; Lev, O. *J. Electroanal. Chem.* **2004**, *565*, 7–19.
 (21) Modestov, A. D.; Gun, J.; Mudrov, A.; Lev, O. *Electroanalysis* **2004**, *16*, 367–378.
 (22) Jurva, U.; Wikstrom, H. V.; Weidolf, L.; Bruins, A. P. *Rapid Commun. Mass Spectrom.* **2003**, *17*, 800–810.
 (23) Losito, I.; Cioffi, N.; Vitale, M. P.; Palmisano, F. *Rapid Commun. Mass Spectrom.* **2003**, *17*, 1169–1179.
 (24) Hayen, H.; Karst, U. *Anal. Chem.* **2003**, *75*, 4833–4840.
 (25) Gun, J.; Modestov, A.; Lev, O.; Poli, R. *Eur. J. Inorg. Chem.* **2003**, *12*, 2264–2272.
 (26) Gun, J.; Modestov, A.; Lev, O.; Saurenz, D.; Vorotyntsev, M. A.; Poli, R. *Eur. J. Inorg. Chem.* **2003**, *3*, 482–492.
 (27) Kertesz, V.; Van Berkel, G. J. *J. Am. Soc. Mass Spectrom.* **2002**, *13*, 109–117.
 (28) Kertesz, V.; Van Berkel, G. J. *Electroanalysis* **2001**, *13*, 1425–1430.
 (29) Zhang, T. Y.; Brajter-Toth, A. *Anal. Chem.* **2000**, *72*, 2533–2540.
 (30) Roussel, C.; Dayon, L.; Rohner, T. C.; Lion, N.; Girault, H. H. *Biophotonics New Frontier: From Genome to Proteome*; Faupel, M. D., Meyrueis, P., Eds.; Proceedings of the SPIE; Strasbourg, France, April 27, 2004; Vol. 5461, pp 30–37.
 (31) Zhang, T. Y.; Palii, S. P.; Eyler, J. R.; Brajter-Toth, A. *Anal. Chem.* **2002**, *74*, 1097–1103.
 (32) Johnson, K. A.; Shira, B. A.; Anderson, J. L.; Amster, I. J. *Anal. Chem.* **2001**, *73*, 803–808.
 (33) Permentier, H.; Poolman, B. *Mol. Cell. Proteomics* **2005**, S349.
 (34) Permentier, H. P.; Jurva, U.; Barroso, B.; Bruins, A. P. *Rapid Commun. Mass Spectrom.* **2003**, *17*, 1585–1592.
 (35) Roussel, C.; Dayon, L.; Lion, N.; Rohner, T. C.; Jossierand, J.; Rossier, J. S.; Jensen, H.; Girault, H. H. *J. Am. Soc. Mass Spectrom.* **2004**, *15*, 1767–1779.
 (36) Prudent, M.; Girault, H. H. *J. Am. Soc. Mass Spectrom.* **2008**, *19*, 560–568.
 (37) Dayon, L.; Roussel, C.; Girault, H. H. *J. Proteome Res.* **2006**, *5*, 793–800.
 (38) Chen, H.; Zhang, Y. H.; Mutlib, A. E.; Zhong, M. *Anal. Chem.* **2006**, *78*, 2413–2421.
 (39) Dayon, L.; Jossierand, J.; Girault, H. H. *Phys. Chem. Chem. Phys.* **2005**, *7*, 4054–4060.
 (40) Roussel, C.; Dayon, L.; Lion, N.; Rohner, T. C.; Jossierand, J.; Rossier, J. S.; Jensen, H.; Girault, H. H. *J. Am. Soc. Mass Spectrom.* **2004**, *15*, 1767–1779.
 (41) Prudent, M.; Roussel, C.; Girault, H. H. *Electrochem. Commun.* **2007**, *9*, 2067–2074.
 (42) Rohner, T. C.; Girault, H. H. *Rapid Commun. Mass Spectrom.* **2005**, *19*, 1183–1190.
 (43) Wang, J. *Stripping Analysis: Principles, Instrumentation, and Applications*; VCH: Weinheim, Germany, 1985.
 (44) Pretty, J. R.; Blubaugh, E. A.; Caruso, J. A. *J. Anal. At. Spectrom.* **1992**, *7*, 1131–1137.
 (45) Pretty, J. R.; Blubaugh, E. A.; Caruso, J. A. *Anal. Chem.* **1993**, *65*, 3396–3404.
 (46) Pretty, J. R.; Caruso, J. A. *J. Anal. At. Spectrom.* **1993**, *8*, 545–550.
 (47) Pretty, J. R.; Blubaugh, E. A.; Caruso, J. A.; Davidson, T. M. *Anal. Chem.* **1994**, *66*, 1540–1547.
 (48) Pretty, J. R.; Duckworth, D. C.; Van Berkel, G. J. *Anal. Chem.* **1998**, *70*, 1141–1148.
 (49) Pretty, J. R.; Van Berkel, G. J.; Duckworth, D. C. *Anal. Bioanal. Chem.* **1998**, *178*, 51–63.

(50) Pretty, J. R.; Van Berkel, G. J. *Rapid Commun. Mass Spectrom.* **1998**, *12*, 1644–1652.
 (51) Baca, A. J.; De La Ree, A. B.; Zhou, F.; Mason, A. Z. *Anal. Chem.* **2003**, *75*, 2507–2511.
 (52) Brisenio, A. L.; Baca, A. J.; Zhou, Q.; Lai, R.; Zhou, F. *Anal. Chim. Acta* **2001**, *441*, 123–134.
 (53) Baca, A. J.; Garcia, Y.; Brisenio, A. L.; Zhou, F. *J. Electroanal. Chem.* **2001**, *513*, 25–35.
 (54) Cao, G. X.; Jimenez, O.; Zhou, F.; Xu, M. *J. Am. Soc. Mass Spectrom.* **2006**, *17*, 945–952.
 (55) Liljegren, G.; Forsgard, N.; Zettersten, C.; Pettersson, J.; Svedberg, M.; Herranen, M.; Nyholm, L. *Analyst* **2005**, *130*, 1358–1368.
 (56) Pretty, J. R.; Deng, H. T.; Goeringer, D. E.; Van Berkel, G. J. *Anal. Chem.* **2000**, *72*, 2066–2074.

signature of avidin was resolved using a high-resolution ESI-MS instrument, a LTQ-Orbitrap (ThermoFisher). The ESI was operated in the positive ion mode with a spray voltage of 1.2 kV, capillary voltage 47 V, and temperature of 200 °C. Mass spectra were obtained by scanning the 600–2000 m/z range with 2 total microscans, and the maximum inject time was 300 ms.

Electrochemical Deposition–Stripping by EC/ESI-MS.

The electrochemical studies were carried out using a CH Instruments model 750B Electrochemical Workstation (Austin TX). The electrochemical flow cell was described in our previous publications. A scheme of the flow cell is provided in the Supporting Information, Figure S-1, and in previous publications.^{20,21} In the current studies we used a thicker cell (of 100 μm thickness) and the working electrode radius was 1 mm. The flow cell volume was 0.24 μL . The total volume from the electrode to the injection needle including tubing was 2.1 μL . The thin-layer radial flow cell was equipped with a Pt working electrode (1.0 mm diameter), and two Ag-wires in 0.1 M AgNO_3 in separate compartments were used as counter and reference electrodes. The reagent solution flow-rate was 2–5 $\mu\text{L}/\text{min}$ for the deposition step and 20–30 $\mu\text{L}/\text{min}$ for the stripping step. All the electrochemical flow tests were conducted with this flow cell. All the ESI-MS spectra were taken online (in EC/ESI-MS mode), except for the high-resolution ESI-MS spectrum of avidin (Figure 8).

Organothiols Preconcentration Tests. Silver was deposited from 1 mM AgNO_3 in 0.5 M H_2SO_4 aqueous electrolyte on a Pt working electrode. The deposition was conducted for 20 min at 0 V vs Ag/AgNO_3 (0.1 M) electrode. The cell was washed and refilled with the 0.5 M NH_4Ac in H_2O ($\text{pH} = 4.0$).

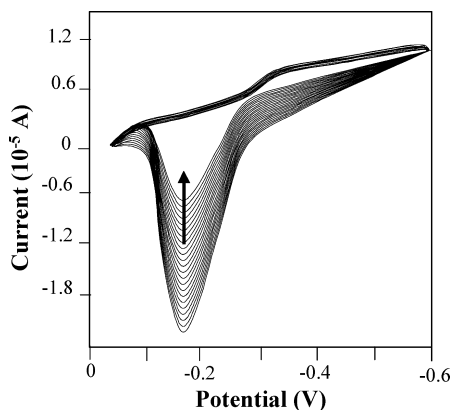


Figure 1. Cyclic voltammetry deposition of homocysteine, 1 mM in 0.5 M NH_4OH , scan rate 50 mV/s.

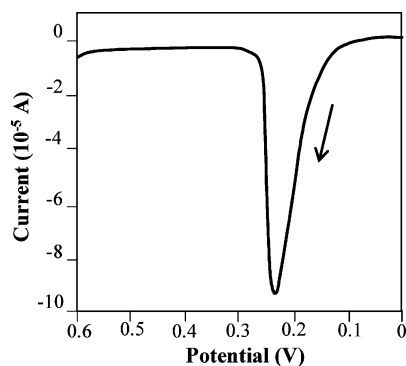


Figure 2. Electrochemical stripping of silver–homocysteine, scan rate 50 mV/s.

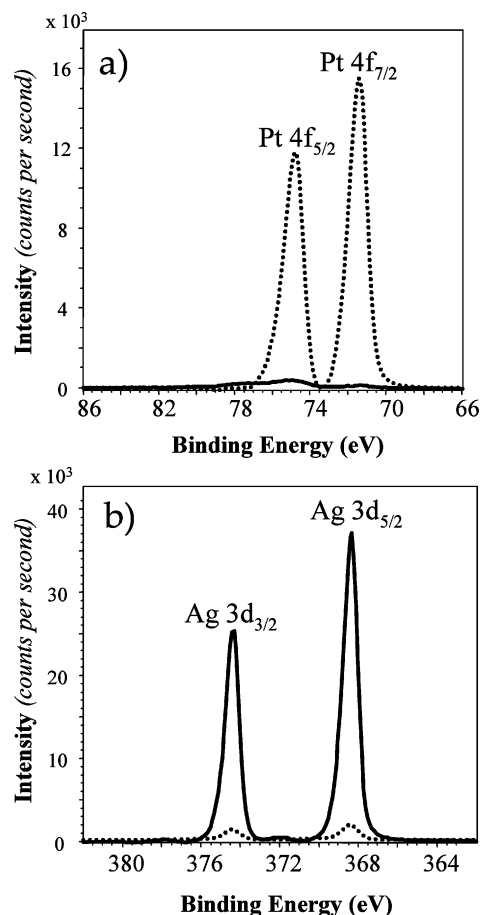


Figure 3. XPS spectra of the Ag-coated Pt-electrode with cysteine electrodeposition before stripping (solid) and after stripping (dashed): (a) Pt 4f level and (b) Ag 3d level.

Organothiol compounds (homocysteine, cysteine, methionine, and mercaptoacetic acid, all 1 mM concentrations in the 0.5 M NH_4Ac in H_2O solution) were electrodeposited on the silver layer by cycling the electrode potential from -0.6 to -0.05 V at 50 mV/s scan rate. After the deposition of the thiols on the electrode surface, the cell was washed with 50:50 MeOH/0.5 M NH_4Ac in H_2O solution (HPLC grade methanol, 99.8% from Baker). At the final stage, the silver deposit along with its coating were stripped from the electrode by a potential sweep from 0 to 0.6 V at 2 mV/s scan rate in 50:50 MeOH/0.5 M NH_4Ac in H_2O ($\text{pH} = 4.0$) electrolyte, and the stream was transferred to the ESI-MS. After each deposition/stripping cycle, the working electrode was cleaned by cycling the potential 10 times between 0 and 0.8 V at 500 mV/s in a stream of 0.5 M NH_4Ac aqueous solution.

Biotin–Avidin Preconcentration. The silver and thiol (homocysteine) were electrodeposited as described before. Subsequently, the cell was washed with 1 mg/mL solution of biotin EZ-Link Sulfo-NHS-Biotin (sulfo-succinimidobiotin) (Pierce Biotechnology, Rockford, IL) in PBS (0.2 M, $\text{pH} = 7$) for 2 h at room temperature at 5 $\mu\text{L}/\text{min}$ flow rate. Reaction of EZ-Link Sulfo-NHS-Biotin with the primary amine of homocysteine results in surface modification with biotin. Then, avidin (ImmunoPure avidin (salt free), Pierce Biotechnology, Rockford, IL) was conjugated to the biotin by flashing the cell with the avidin solution containing 1 mg/mL avidin in 50 mM NH_4Ac ($\text{pH} = 7$) for 2 h at a flow rate

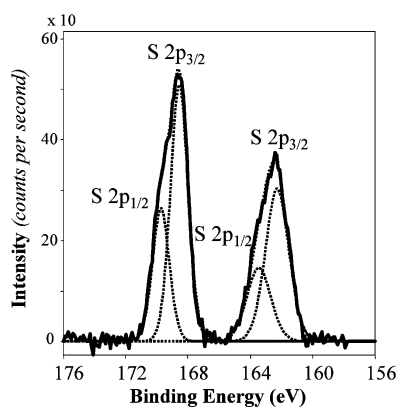


Figure 4. XPS S 2p level spectra of cysteine, electrodeposited on silver (and the deconvoluted peaks). The lower peak (162.3 eV) corresponds to the cysteine bound to silver, and the higher peak (168.6 eV) corresponds to oxidized sulfur.

of 5 $\mu\text{L}/\text{min}$. Between each step, the cell was washed with 50:50 MeOH/0.5 M NH_4Ac in aqueous solution. Silver stripping was done with 50:50 MeOH/0.5 M NH_4Ac in H_2O (pH = 4.0) by scanning the potential from 0 to 0.6 V (2 mV/s) at a flow rate of 20 $\mu\text{L}/\text{min}$.

Electron Microscopy and X-ray Photoelectron Spectroscopy. In order to carry out scanning electron microscopy (SEM) and X-ray photoelectron spectroscopy (XPS) measurements of the modified electrodes, we used an electrochemical cell equipped with a miniature retractable electrode. After the deposition or stripping, the electrode was pulled out and introduced to the vacuum chamber of the SEM or XPS without any further modification. For XPS analyses, overnight pumping was used to achieve ultrahigh vacuum conditions.

XPS measurements were performed on a Kratos Axis Ultra X-ray photoelectron spectrometer. Spectra were acquired with monochromated Al $K\alpha$ (1486.7 eV) X-ray source with a 0° takeoff angle. The pressure in the test chamber was maintained at 1.5×10^{-9} Torr during the acquisition process. The high-resolution XPS scans were acquired for C 1s, S 2p, Ag 3d, and Pt 4f peaks with a pass energy of 20 eV and step size of 0.1 eV. The XPS binding energy was calibrated with respect to the peak position of C 1s as 285.0 eV.⁵⁷ Data analysis and processing were performed with Vision processing data reduction software (Kratos Analytical Ltd.) and CasaXPS (Casa Software Ltd.).

SEM imaging and analyses were performed using the FEI Quanta 200 environmental scanning electron microscope, equipped

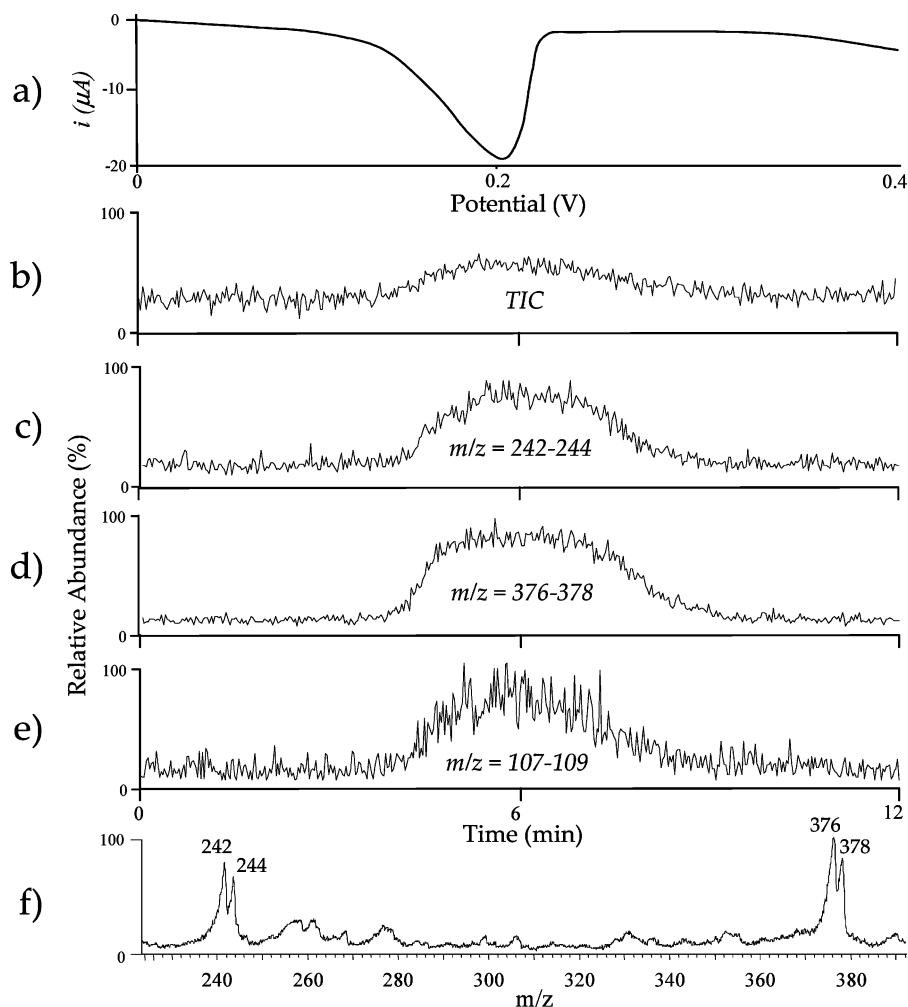


Figure 5. Online, time trace of selected ions and TIC of silver-homocysteine stripping from an electrode prepared from 1.0 mM homocysteine coating solution (in 0.5 M NH_4Ac , flow rate 25 $\mu\text{L}/\text{min}$, scan rate = 2 mV/min): (a) Ag-homocysteine stripping voltammogram (from 0 to 0.4 V and back); (b) time trace of total ions current (TIC); (c–f) potential dependence of the relative abundance of product ions (c) $m/z = 242-244$; (d) $m/z = 376-378$; (e) $m/z = 107-109$; and (f) ESI-MS spectra with two main product ions, 242–244 and 376–378, taken at $E = 0.2$ V.

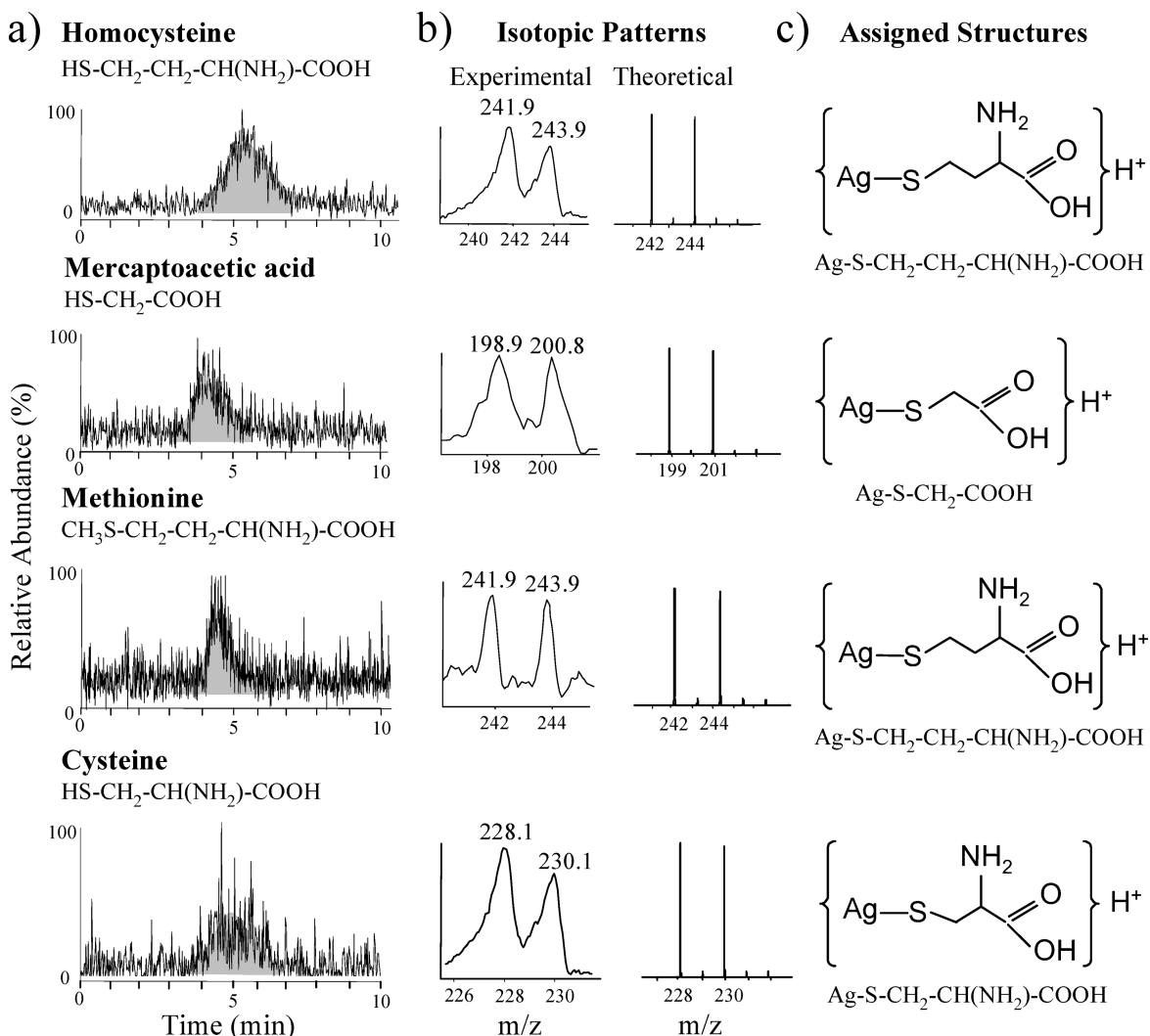


Figure 6. EC/ESI-MS of different thiols. Column a is the extracted ion time traces during electrostripping of different organothiols. Desorption conditions are depicted in Figure 5. The MS was operated in scan mode over the 50–500 amu range. The respective time traces correspond to the extracted ion time trace over the period of 3 min: 241–245 for homocysteine, 198.5–201.5 for mercaptoacetic acid, 241.5–244.5 for methionine, and 227–231 for cysteine. Column b is the expanded isotopic patterns of the stripping product (experimental and theoretical). Column c is the assigned structures of the products.

with an EDAX energy dispersive X-ray spectroscopy system (spectral resolution 128 eV). The acceleration voltage was 15.0 kV, the working distance was 12 mm, and the spectra acquisition time was set for 50 s.

RESULTS AND DISCUSSION

Silver Electrodeposition. Silver deposition on platinum electrodes was described in several articles.^{58,59} In this study, we used the underpotential deposition of silver at $E = 0.0$ V, largely following the research of the groups of Vaskevich and Gileadi^{60–62} and Avaca.⁶³ The dependence of the stripping peak area on deposition time and potential is demonstrated in Figure S-2a,b of the Supporting Information. The presence of the silver layer on the electrode was confirmed by SEM imaging and EDAX analyses which are presented in Figure S-3 of the Supporting Information.

Thiols Electrodeposition and Stripping. The electrochemical adsorption of the alkanethiols on silver was extensively studied in the past showing that dense packing of alkanethiols can be obtained. In fact, denser packing was reported for alkanethiols on silver than on other precious metals.⁶⁴ Jennings and Laibins⁶⁵

studied electrodeposition of alkanethiols on silver film that was deposited by underpotential deposition. The authors showed that a stable film and full coverage of the underlayer could be achieved.

The cyclic voltammetry of the homocysteine deposition on silver modified Pt electrode is shown in Figure 1. The potential was cycled at 50 mV/s from $E = -0.6$ V to $E = 0.0$ V, i.e., before the range of silver oxidation–dissolution. By deposition of thiols on the silver, we could concentrate these compounds on the electrode surface and then, by fast electrochemical oxidation of the silver, to dissolve thiol-containing compounds and transfer them to the MS. Figure 2 demonstrates the oxidative stripping peak of silver which appears at $E = 0.2$ – 0.3 V.

XPS Studies of Thiol Deposition on a Silver Coated Electrode. The organothiol (cysteine) was electrodeposited on the silver-plated Pt electrode as described in the Experimental Section, and the electrode was analyzed by XPS before and after silver stripping (Figure 3). Before stripping (solid lines), the platinum electrode shows silver coverage; therefore, the Pt signal (Pt 4f_{7/2} position is equal 71.2 eV⁵⁷) is very low, although the

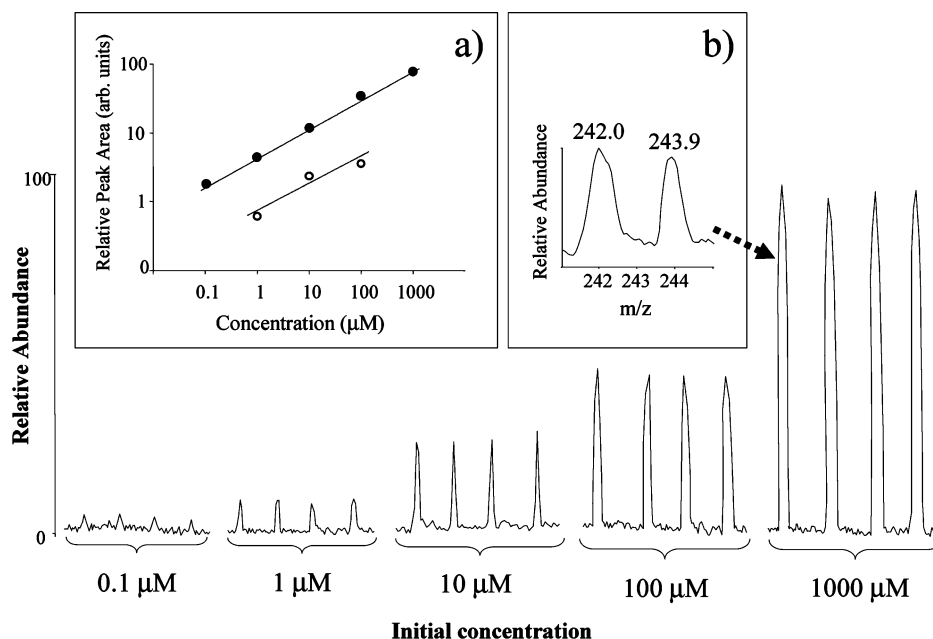


Figure 7. Dose response of homocysteine after electrodeposition and stripping ($m/z = 242-244$). Main figure: Time trace of repeated analysis from different homocysteine concentrations (SIM mode). Inserts: (a) relative peak area vs initial homocysteine concentrations (upper line) and the corresponding calibration curve for optimized injection of homocysteine without preconcentration (lower line) and (b) the experimental isotopic pattern. The repeatability-based error bars are smaller than the size of the symbols.

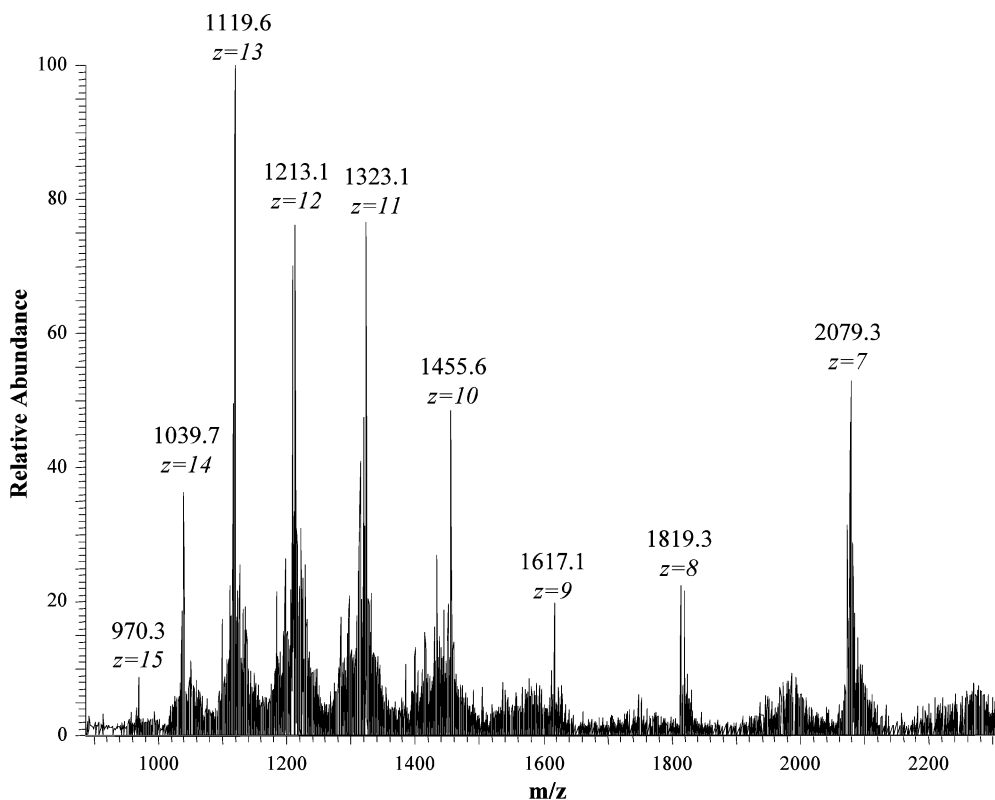


Figure 8. High-resolution ESI-MS spectra of multicharged avidin monomer ($z = 7-15$). The total molecular mass of protein monomer is 14 556 amu.

Ag signal (Ag $3d_{5/2}$ position at 368.3 eV⁵⁷) is high. After the stripping, the silver was removed; hence, the Pt 4f signals increase and the Ag 3d decrease.

Chemisorbed cysteine could be recognized by two sulfur peaks (S 2p level) as shown in Figure 4. The S 2p peaks show a 1.18 eV gap between S $2p_{3/2}$ and S $2p_{1/2}$, and the doublets intensity ratio is

2:1. The lower doublet at S $2p_{3/2} = 162.3$ eV is associated with cysteine bound to the silver. The position of this peak agrees well with previously reported binding energies 162.4 eV for thiol bound to silver.⁶⁶ The binding energy of free cysteine is 163.0 eV.⁶⁷ The higher S $2p_{3/2}$ peak at 168.6 eV is assigned to oxidized sulfur impurities, following previously reported assignment.⁶⁶

EC/ESI-MS Studies. Coupled EC/ESI-MS studies were conducted during stripping potential sweeps between $E = 0.0$ V to $E = 0.6$ V at the 2 mV/s rate. The silver has two main isotopes, 107 and 109 with almost equal abundance. Hence, the observed silver–thiol complexes may be distinguished by their characteristic isotope patterns exhibiting two main peaks with a 2 amu gap. Homocysteine (methylcysteine) preconcentration was selected as a test case. Figure 5 shows the time (or potential) trace of the different species during silver electrostripping. The upper curve (Figure 5a) depicts the hydrodynamic (cyclic) voltammetry recorded simultaneously with the ESI-MS time-dependent spectra (Figure 5b–e). Figure 5b depicts the development of the total ion current (TIC) as a function of stripping potential. It can be seen that silver stripping substantially increases the total ion intensity. The peak of this increase coincides with the electrochemical stripping peak, and it was synchronized with it in time. The lower curves (Figure 5c–e) show the evolution of the specific reaction products of the oxidative stripping. The evolution of $m/z = 107$, 109 (Figure 5e) corresponds to the silver ion. The two peaks with $m/z = 242$, 244 were assigned to a complex of Ag and homocysteine $[\text{Ag}-\text{S}-\text{CH}_2-\text{CH}_2-\text{CH}(\text{NH}_2)-\text{COOH}]\text{H}^+$. The peaks at $m/z = 376$ and 378 were assigned to $[\text{Ag}(\text{S}-\text{CH}_2-\text{CH}_2-\text{CH}(\text{NH}_2)-\text{COOH})_2]\text{H}^+$. Homocysteine itself, its protonated forms, and its oxidized dimer were not observed.

Identification of Various Organothiols by Electrodeposition and Stripping. The electrochemical preconcentration and stripping coupled with ESI-MS could be applied for other thiols as well. Figure 6 presents time trace of four different thiols: homocysteine, cysteine, methionine, mercaptoacetic acid by the deposition–stripping ESI-MS analyses (the experimental conditions are same as in the previous part). Figure 6 also presents the assigned peaks of the different organothiols after their preconcentration on silver, the experimental and theoretical isotope patterns, and the assigned structures. Theoretical spectra were calculated with the IsoPro 3.0 Software.⁶⁸

Dose Response. The data presented thus far was taken in a broad range scan mode to demonstrate the speciation/identification power of the EC/ESI-MS. However, better quantitative information can be gained in the selected ion monitoring (SIM) mode. The relation between the initial thiol concentration and the stripping signal was studied for different concentrations of homocysteine. In these experiments, we followed the time trace of

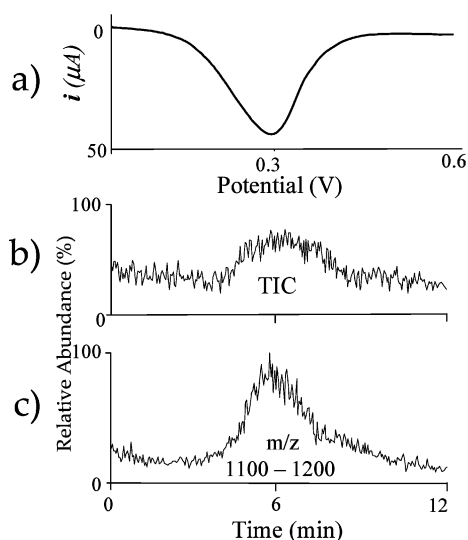


Figure 9. Online EC/ESI-MS time trace of the Ag–homocysteine–biotin–avidin set: (a) hydrodynamic voltammetry curve, (b) total ion current (TIC) of the potential sweep (500–4000 amu), and (c) evolution of the stripping signal, corresponding to avidin monomer.

the 243 m/z ion with a 4 amu mass width, encompassing the m/z of 242 and 244 of the silver thiol adduct (Figure 5). The injection to the MS was done at a flow rate of 1 mL/min with MeOH as the auxiliary solvent. Figure 7 depicts the time traces of extracted ions of the 242–244 amu range for different concentrations of homocysteine. A minimal detection limit at a signal-to-noise = 5 was 0.1 μM . The dynamic range spans the range 0.1–1 000 μM in a logarithmic scale. Figure 7a illustrates the dependence of the relative abundance peak area of the silver–thiol complex ($m/z = 242$ –244) on the concentration of homocysteine in the electrodeposition solution. Standard deviations based on 4 injections at different concentrations were 8% for 0.1 μM , 5% for 1 μM , 14% for 10 μM , 11% for 100 μM , and 7% for 1000 μM , the repeatability was evaluated also by 17 repeated tests of 1 mM homocysteine giving 7.6% relative standard deviation. For comparison, direct injection of homocysteine under optimized conditions shows an order of magnitude lower response, and the minimum detection limit at a signal-to-noise = 3 was 1 μM . A human blood plasma test which is outlined in the Supporting Information (Figure S-4) showed proof of principle for biological applications.

Selective Preconcentration for Biochemical Applications.

EC/ESI-MS enrichment on a predeposited silver layer and electrochemical stripping can be used for specific (biochemical) analysis as well. In this example, a target protein, avidin was preconcentrated for analysis by formation of a surface confined biotin–avidin complex. The first stage of electrode preparation was identical to the organothiol enrichment protocol. We first deposited silver and then bonded the homocysteine onto it. At the next step, the biotin was coupled to the surface attached homocysteine by Sulfo-NHS-Biotin (sulfosuccinimidobiotin of Pierce). For that, the biotin was pumped through the cell for 2 h at a low flow rate of 1 $\mu\text{L}/\text{min}$. At the final step, avidin was ligated to the biotin by pumping the avidin containing solution (1 mg/mL in 10 mM NH_4Ac in H_2O) at a low flow rate (1 $\mu\text{L}/\text{min}$) through the cell.

Figure 8 presents the avidin signal from a solution containing 1 mg/mL (25 mM NH_4Ac , $\text{H}_2\text{O}/\text{MeCN}$ 50:50), which

- (57) Moulder, J. F.; Stickle, W. F.; Sobol, P. E.; Bomben, K. D. *Handbook of X-ray Photoelectron Spectroscopy*; Physical Electronics Inc.: Eden Prairie, MN, 1992.
- (58) Attard, G. A.; Al-Akl, A. J. *Electroanal. Chem.* **2003**, 554–555, 439–448.
- (59) Ramirez, C.; Arce, E. M.; Romero-Romo, M.; Palomar-Pardave, M. *Solid State Ionics* **2004**, 169, 81–85.
- (60) Vaskevich, A.; Rosenblum, M.; Gileadi, E. *J. Electroanal. Chem.* **1994**, 383, 167–174.
- (61) Vaskevich, A.; Rosenblum, M.; Gileadi, E. *J. Electroanal. Chem.* **1996**, 412, 117–123.
- (62) Vaskevich, A.; Gileadi, E. *J. Electroanal. Chem.* **1998**, 442, 147–150.
- (63) Mascaro, L. H.; Santos, M. C.; Machado, S. A. S.; Avaca, L. A. *J. Chem. Soc., Faraday Trans.* **1997**, 93, 3999–4003.
- (64) Mohtat, N.; Byloos, M.; Soucy, M.; Morin, S.; Morin, M. *J. Electroanal. Chem.* **2000**, 484, 120–130.
- (65) Jennings, G. K.; Laibinis, P. E. *J. Am. Chem. Soc.* **1997**, 119, 5208–5214.
- (66) Majid, A.; Bednaseba, F.; L'Ecuier, P.; Deslandes, Y. *Rev. Adv. Mater. Sci.* **2003**, 4, 25–31.
- (67) Llopiz, P.; Maire, J. C. *Bull. Chim. Soc. Fr.* **1979**, 11, 457–462.
- (68) Senko, M. *Iso Pro 3.0 MS/MS Software. Isotopic Pattern Simulator*; National High Magnetic Field Laboratory: Sunnyvale, CA, 2002.

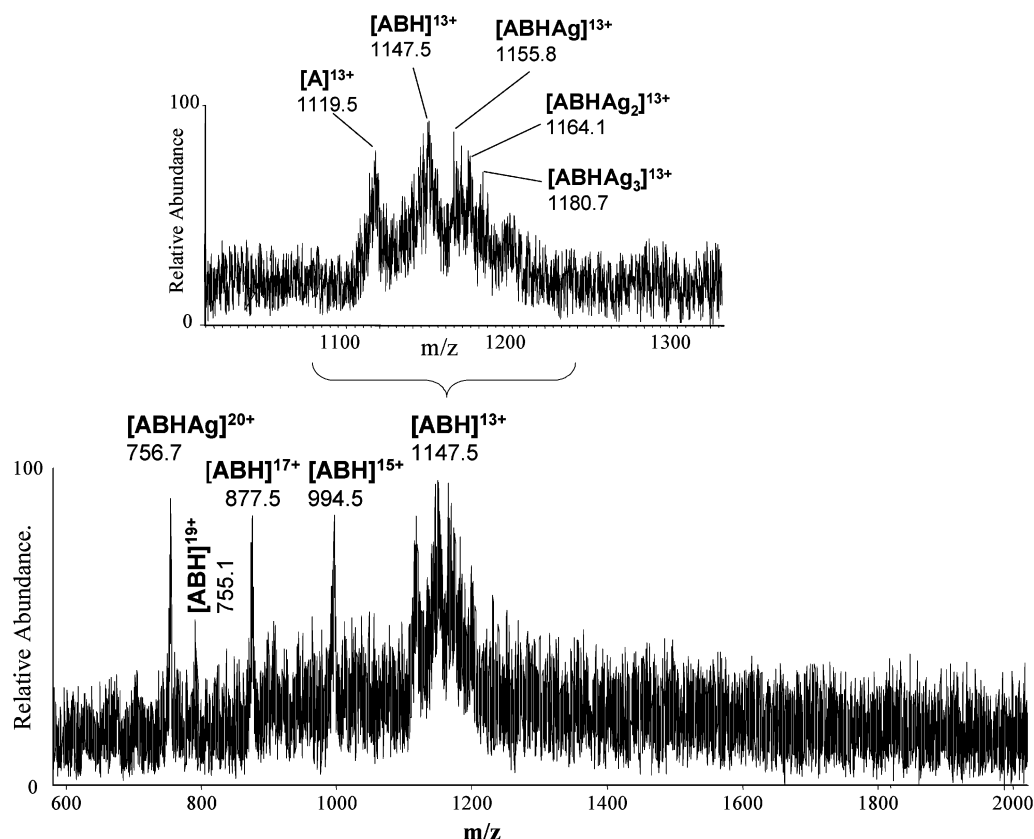


Figure 10. ESI-MS signal of the electrochemically stripped avidin-biotin-homocysteine. Lower frame: full range MS signal (500–2000 amu) showing the protein complex peaks which correspond to multicharged avidin-biotin-homocysteine complex $[ABH]^{13+}$ ($z = 13$) at 1147.5 amu, $[ABH]^{15+}$ at 994.5, $[ABH]^{17+}$ at 877.5, $[ABH]^{19+}$ at 755.1, and the complex avidin-biotin-homocysteine-Ag $[ABHAg]^{20+}$ at 756.7. Upper frame: expanded MS range with several peaks corresponding to different avidin-biotin-homocysteine-Ag complexes: avidin $[A]^{13+}$ at 1119.5, avidin-biotin-homocysteine $[ABH]^{13+}$ at 1147.5, avidin-biotin-homocysteine-Ag $[ABHAg]^{13+}$ at 1155.8, $[ABHAg_2]^{13+}$ at 1164.1, and $[ABHAg_3]^{13+}$ at 1180.7.

comprises several multiprotonated protein peaks ($z = 7$ –15) obtained using a high-resolution ESI-MS instrument, LTQ-Orbitrap (ThermoFisher). The total mass of the protein was calculated to be 14 556 amu corresponding to one monomer of the avidin tetramer. This attests that under these ESI conditions the avidin tetramer is cleaved to its monomeric building blocks.

Figure 9 delineates the electrochemical and the (LCQ classic) ESI-MS time trace signals resulting from electrostripping of the silver along with its surface bound homocysteine-biotin-avidin set. The upper curve represents the hydrodynamic voltammetry with Ag stripping peak at 0.3 V. Figure 9b shows the TIC which increases during the stripping. Figure 9c corresponds to the avidin-biotin complex signal. In Figure 10, we can distinguish several avidin-biotin-homocysteine-Ag fragments with the same charge ($z = 13$). The protein signal corresponding to $z = 13$ (1119.5) is also the most intense in the high-resolution pure protein spectra (Figure 8), and it is the only one that was observed in the (LCQ classic) EC/ESI-MS test. The mass 1147.5 relates to the avidin-biotin-homocysteine complex. The 1155.8 was assigned to the avidin-biotin-homocysteine-Ag complex. The peaks at amu = 1164.1 and 1180.7 correspond to the avidin-homocysteine complex with two and three silver atoms, respectively (Figure 10).

The avidin concentration-stripping test shows a proof of concept of a generic electrochemically controlled precon-

centration-stripping approach. The process is generic from several points of view: A change of ligating agent will concentrate other analytes. Naturally the analytes are not necessarily proteins or peptides and can also be chemical or biochemical entities, provided they can be accumulated (specifically or nonspecifically) on a ligating agent bound to the electrode. The method is not limited by analyte size either, and in this case a 60k amu protein could be analyzed (though in fact only the monomer is observed). Moreover the current protocol is very general and can be extended to other electrodeposited thin films including copper tagging of proteins as suggested by the Girault group^{35,36} by concentrating the analyte to a ligand bound on an electrodeposited thin copper film. The approach is not limited to the concentration of a single analyte. Several analytes can be concentrated on the same electrode by attaching several chelating agents on the same electrode or by using less specific ligands. Moreover, an array of electrodes can be used to selectively bind different analytes on different electrodes, and the electrode elements can be electrostripped sequentially to the ESI-MS. Although the density of such an array cannot approach that of SELDI-TOF, the approach can be useful for array electroscreening of analytes that require ESI-MS interfacing.

CONCLUDING REMARKS

We introduce a new approach for electrochemically induced analytes' introduction to the electrospray mass spectrometer based

on electrochemical concentration of analytes on under potential deposited (UPD) silver and subsequent electrostripping of the silver and the deposited analyte to an online electrochemical flow cell.

The electrochemical deposition–stripping method, coupled with online ES-MS can be successfully used for determination of various thiols. A generic method based on this feature and inspired by SELDI-TOF was introduced for electrospray ionization MS analysis of target (bio)analytes. As in SELDI-TOF, the target compound is captured by surface bound ligands, but in this process electrochemical dissolution of the supporting surface dissolves the analytes and facilitates their delivery to an online ESI-MS. We have little faith that the algorithm will achieve the spatial resolution of SELDI-TOF but it shares a common feature: spatially addressable analysis of selectively captured analytes. The method can be generalized for the analyses of an array of electrodes each concentrating and individually electrostripping a different captured analyte.

ACKNOWLEDGMENT

We thank O. Moshel for high-resolution ESI-MS analysis of protein and the Unit for Nanocharacterization of the Center for Nanoscience and Nanotechnology, The Hebrew University, Jerusalem, for SEM and XPS analyses. The authors thank the Israel Science Foundation for partial finance of this research.

SUPPORTING INFORMATION AVAILABLE

Additional information as noted in text. This material is available free of charge via the Internet at <http://pubs.acs.org>.

Received for review June 14, 2009. Accepted August 20, 2009.

AC901285M